Properties of moiré magnifiers

Hala Kamal*
Reinhard Völkel**
Javier Alda*

* Departamento de Optica
Universidad Complutense de Madrid.
Facultd de Físicas.
Ciudad Universitaria
s/n-28040 Madrid, Spain
Phone: +34.1.394.4555;
Fax: +34.1.394.4674
E-mail: j.alda@fis.ucm.es

** Institute of Microtechnology
Université de Neuchâtel,
Rue A.-L. Breguet 2
CH-2000 Neuchâtel, Switzerland
Phone: +41.32.718.3279;
Fax: +41.32.718.3201
E-mail: reinhard.voelkel@imt.unine.ch

1 Abstract:

Moiré magnification can be observed visually if an array of identical objects is viewed through an array of identical microlenses with a different period. Theoretical analysis and experimental results of the moiré image obtained by moiré magnifier are presented. Conditions for erect and inverted moiré magnifications are derived and interpreted. Virtual erect images are observed only when the period of the lens array is larger than that of the object array, while inverted images are obtainable in both cases. For equal periods, uniform field of view results. The relation between the relative size of the periods and the distance between object and lens array are derived. Expressions for image magnification, orientation and size are deduced. The condition to obtain a demagnified moiré pattern is deduced. Rotation of the lens array with respect to the object array results in rotation of the erect and inverted moiré pattern in similar and opposite directions, respectively.

Subject terms: Moiré effect, microlens arrays

2 Introduction

The term moiré is a French word meaning 'watered mohair', a glossy cloth with wavy alternating patterns that change forms as the wearer moves. It is also referred to the 'watery and wavy' appearance when layers of silk are pressed together by special techniques[1]. Physically it is an optical phenomenon resulting from the superposition of two or more periodic grid structures. The resulting moiré pattern is influenced by changing any of the three geometrical parameters characterizing the individual grid structures, namely, period, orientation and shape.[1, 2, 3]

Although there is a long history in the investigation of superposition moiré effects, only few publications exist which describe the moiré effects appearing if a periodic array of identical objects is observed through a periodic microlens array.[4, 5] However, this moiré magnification effect, as the authors of this article call the phenomenon, is well known from integral images and integral photography.[6, 7] The frequent appearance of similar phenomenon in the usage of microlens array in conjunction with arrays of light sources, photo-detectors, liquid crystals displays, CCD-chips, etc. motivates to further investigations about this phenomena.[8]

The term 'moiré magnifier' is suggested by the conjunction of a periodic object seen through a periodic array of optical elements or systems. The image is formed as the composition, side by side, of the individual images generated by the optical array. The image formation is equal to superposition compound eyes as nocturnal insects and deep-water crustaceans have.[9] The foundations of optical array design also demonstrate the existence of cooperative effects.[10] In optical array design, the composed image is named as the synthetic image. By using this last approach, the 'moiré magnifier' system should be named as 'synthetic magnifier'. However, we prefer to keep the term 'moiré magnifier' because of the good acceptance of this term by the optics community after the presentation of the device by Hutley et. al..

The article from Hutley et. al. [4] dealt with an object array combined with a lens array whose period is nearly the same size. Experimental results for the magnification and orientation of moiré images and their fundamental dependence on the orientation of the lens array have been given. In our investigation, we explain the formation of erect and inverted moiré images for moiré magnifier consisting of microlens and object arrays with different periods. We derive the relation between the relative period difference of the arrays and the object array position in x, y, z and θ. We describe the rotation properties of moiré magnifiers.

3 Basic properties of a moiré magnifier

The basic configuration of a moiré magnifier is shown in Figure 1. An array of identical objects (Figure 1-b) is imaged by an array of identical lenses (Figure 1-c). For certain combinations of object and lens arrays, one or more magnified moiré images of the object motif are observed (Figure 1-d). We will now derive the general properties of moiré magnification. For simplicity, we restrict our investigation on symmetrical square arrays. However, a variety of different array types (hexagonal, rhombic, etc.) might be used for moiré magnification in a similar way.

The object array shown in Fig. 1 consists of $O \times O$ identical objects or motifs at a period Λ_O. The lens array consists of $L \times L$ identical lenses of $\varnothing_L$ aperture at a period Λ_L. The focal length of the lenses is $f > 0$ (positive lens). Each lens images a part of the object array. The actual type or shape of the lenses (circular or square aperture, refractive or diffractive lens, etc.) is not relevant for our investigation. We assume that the lens size is equal to the lens period $\varnothing_L = \Lambda_L$, and ignore all rays not hitting the lenses. The plane of the object array is parallel to the plane of the lens array.

The distance between the object plane and the lens array is s_o. The period of the object array is different from the lens period $\Lambda_O \neq \Lambda_L$. The moiré image is either observed on a screen located at s_i or visually in any plane behind the lens array.
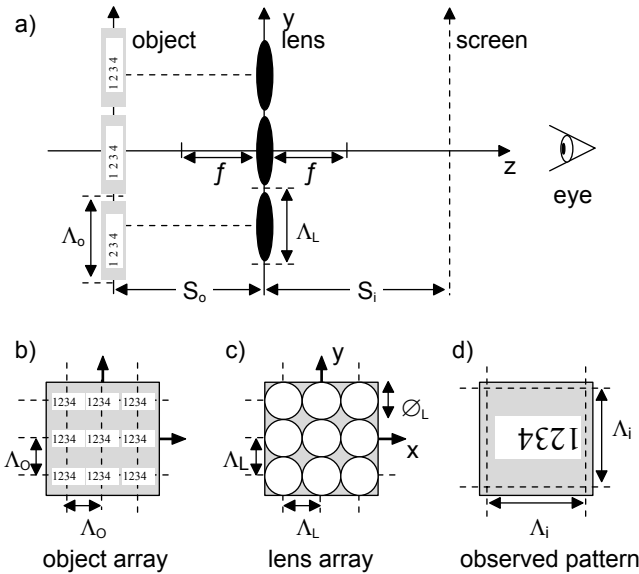

Figure 1. Basic configuration of a moiré magnifier. A symmetric square array of identical objects is imaged by a symmetric square array of identical lenses. The object pitch is Λ_O, the lens aperture $\varnothing_L$, and the lens pitch Λ_L. The distance between object plane and lenses is s_o. The moiré pattern is either observed on a screen located in the image plane at s_i or visually in any plane behind the lens array.
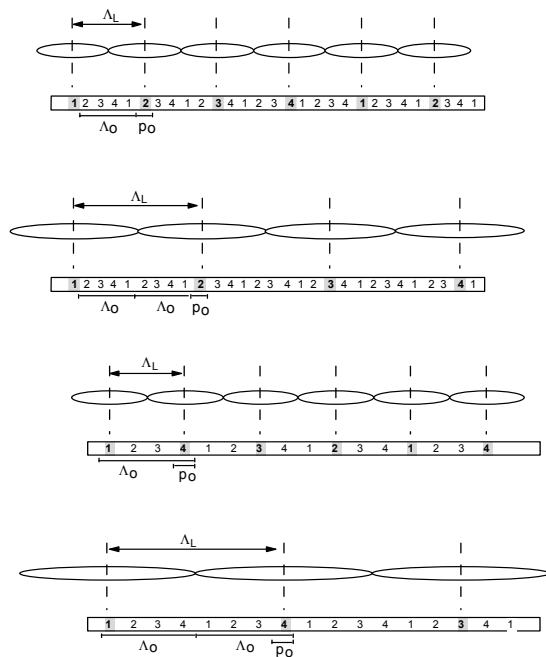

Figure 2. Examples for an object motif consisting of '1234'. If one lens images the '1', the next neighbor lenses (left and right) should image the '4' or '2' to generate a complete moiré image of the object motif. However, the '4' or '2' portion might be next to '1' or at a certain distance.

The first fundamental condition for moiré magnification requires that adjacent lenses image adjacent portions p_o from the object motif. Figure 2 shows exam-

ples for an object motif consisting of '1234'. If one lens images the '1', the next neighboring lenses (left and right) should image the '4' or '2' to generate a complete moiré image of the object motif. However, the '4' or '2' portion might be next to '1' or at a certain distance.

An object portions p_o corresponds to an image of the size $p_i = p_o \cdot m$, wherein m is the magnification factor. Images of different object portions combine to form I × I magnified moiré images.

The size of an object portion p_o imaged by one lens is given by

$$p_o = \Lambda_o \frac{I}{L}, \qquad (1)$$

wherein $(L/I)^2$ is the number of lenses required to generate a complete moiré image of the object motif (for square arrays). In order to ensure a coincident superposition of all partial images, the image size p_i should be equal to the lens period Λ_L.

$$|p_i| = \Lambda_L. \qquad (2)$$

The relation between the image size p_i, the object portion p_o and the position of the object array s_o is given by the image equation,

$$m = \frac{p_i}{p_o} = \frac{\pm \Lambda_L}{p_o} = -\frac{f}{s_o - f}, \qquad (3)$$

wherein f is the focal length.[6] Figure 3 illustrates the imaging properties of a single positive lens. As a consequence of Equation (2) and (3), the marginal rays marked as line 1 and line 2 in Figure 3 define the object size p_o. Line 3 and line 4 define the image size p_i. Depending on the object distance s_o the image p_i is either erect ($f > s_o > 0$; m > 1) or inverted ($s_o > f$; m < 0). For an object position $0 < s_o < 2f$, the image p_i is magnified ($|m| > 1$), for $s_o > 2f$, the image is demagnified ($0 < |m| < 1$).

We obtain four different types of moiré image as shown in Table 1.

	Figure 2a	Figure 2b
$f > s_o > 0$; $p_i = + \Lambda_L$; erect image	**1 2 3 4 1 2** *(I)* moiré image **=** object motif	**4 3 2 1 4 3** *(II)* moiré image ° object motif
$s_o > f$; $p_i = - \Lambda_L$; inverted image;	ƚ Ɛ ㄣ ㄥ ƚ Ɛ *(III)* moiré image ° object motif	ㄣ Ɛ ㄥ ƚ ㄣ Ɛ *(IV)* moiré image **=** object motif

Table 1. Different types of superimposed moiré images. Depending on the object position s_o, the image parts p_i = 1, 2, 3, 4 might be erect or inverted. Only in case (I) and (IV), the moiré image is identical to the object motif.

Depending on the object position s_o, the image part p_i might be virtual erect or real inverted. Depending on the difference in period of Λ_O and Λ_L the image sequence might be direct or reversed. Therefore, we obtain four different types of moiré images as shown in Table 1.
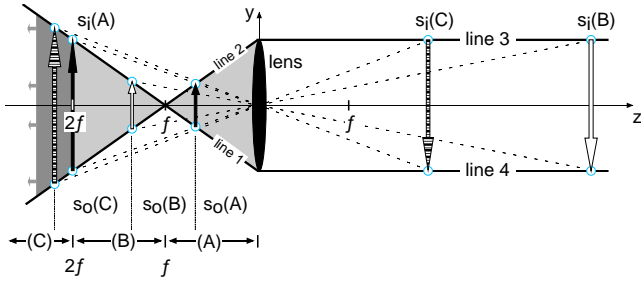
Figure 3. Imaging properties of a single lens of the lens array shown in Figure 1. Three different object positions are possible. (A) The object is located at a distance $|f| > |s_o(A)| > 0$ and generates a virtual, erect image (m > 1) at a distance $s_i(A)$. (B) The object is located at a distance $|2f| > |s_o(B)| > |f|$ and generates a real, inverted image (m < -1) at a distance $s_i(B)$. (C) The object is located at a distance $|\infty| > |s_o(C)| > |2f|$ and generates a real, inverted image (-1 < m < 0) at a distance $s_i(C)$.

Only in case (I) and (IV) the appearing moiré image is identical to the object motif. A graphical explanation of moiré imaging is shown in Figure 4.
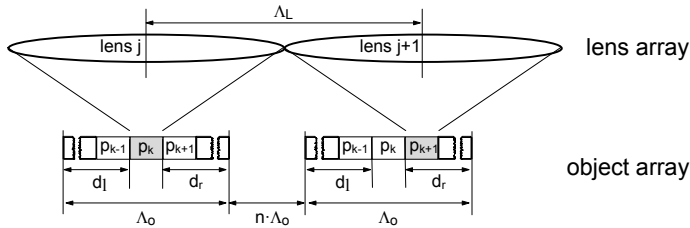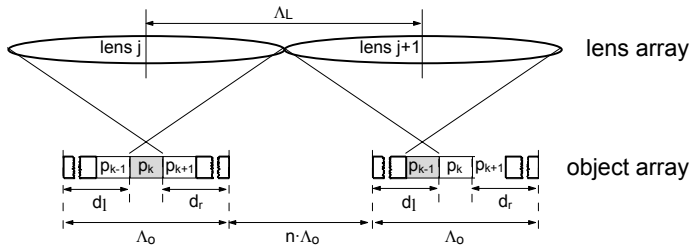

Figure 4. Formation of the (a) erect and (b) inverted moiré images. An object array of period Λ_O is partially imaged by a lens array of period Λ_L. $n\Lambda_O$ is the distance between two arbitrary objects parts participating in building up the moiré image, n, is an integer number (n ≥ 0). Let the object be divided into equal portions of size p given by the image equation (3). d_r is the distance from the right of p_k to the right end of the object element. d_l is the distance from the left of p_k to the left end of the same object element. In Figure 4-a for erect moiré imaging, the two arrays are separated by a distance $f > s_o > 0$. The lens (j) images the kth portion p_k of the first participating object. The lens of order (j+1) images the portion p_{k+1} from the next participating object. In Figure 4-b for inverted moiré imaging, the two arrays are separated by a distance $\infty > s_o > f$. The lens (j) images the kth portion p_k of the first participating object. The lens of order (j+1) images the portion p_{k-1} of the next participating object.

4   The erect moiré pattern

For virtual erect images, the object array is located at a distance $f > s_o > 0$. Each lens forms a virtual erect image of the related object portion p_o as shown in Figure 4-a. If lens (j) images the portion p_k of the object, the next lens of order (j+1) should image the portion p_{k+1}

from the next participating object. The size of p_k is equal to p_{k+1}. Since the size of the image portion p_i is equal to the lens period Λ_L (Equation 2), the distance between two imaged portions is equal to Λ_L given by:

$$\Lambda_L = p_k + d_r + p_k + d_\ell + n\Lambda_O \qquad (4)$$

where, $n\Lambda_O$ is the distance between two participating objects, d_l and d_r are non-imaged parts of the object related to lens j, and n is an integer number (n ≥ 0). Since one object period is given by $\Lambda_O = p_k + d_r + d_l$, the size of the object portion p_{erect} for erect moiré imaging is given by,

$$p_{erect} = \Lambda_L - N\Lambda_O \qquad (5)$$

where, N = n + 1 is an integer number (being ≥ 1). For all values of s_0 in the range $f > s_o > 0$, the size of the object portion p_{erect} is less than the period of the lens array, $0 < p_{erect} < \Lambda_L$, giving m > 1. Substituting in the above inequality from Equation (3), the limits of the integer N for the erect magnified moiré pattern is obtained as,

$$0 < N_{erect} < \frac{\Lambda_L}{\Lambda_O} . \qquad (6)$$

Erect magnified moiré images are only observed if the lens period Λ_L is larger than object period Λ_O. Each value of N corresponds to a different moiré magnification at a different object array position s_o.

5   The inverted moiré pattern

The second case to be analyzed is the condition for obtaining inverted moiré images. The problem is treated in a similar way as that for erects moiré images. For inverted images, the object array is located at a distance $\infty > s_o > f$. As shown in Figure 4-b, each lens images the related object portion p_o. If lens (j) images the portion p_k of the object array, the next lens (j+1) should image the portion p_{k-1} from the next participating object. The size of the image portion p_i is equal to the lens period Λ_L (Equation 2) and given by

$$\Lambda_L = d_r + d_\ell + n\Lambda_O, \qquad (7)$$

where, $n\Lambda_O$ is the distance between two participating objects, d_l and d_r are the non-imaged parts of the object related to lens j, and n is an integer number (n ≥ 0). The integer number n gives the number of not-participating objects in-between two participating objects. Since one object period is given by $\Lambda_O = p_k + d_r + d_l$, the size of the object portion $p_{inverted}$ for inverted moiré imaging is given by,

$$p_{inverted} = N\Lambda_O - \Lambda_L, \qquad (8)$$

where, N = n + 1, is an integer number (being ≥ 1). The condition for inverted moiré imaging is $\infty > s_o > f$. As shown in Figure 3, the size of the object portion p_o is defined by line 1 and 2. Three different object positions s_o are possible:

a)   For $2f > s_o > f$, the size of the object portion is less than the pitch of the lens array, $0 < p_o < \Lambda_L$, leading to m < -1. Substituting for p_o from relation (8), the

limits of the integer N≥1 for the inverted magnified moiré pattern is obtained as,

$$\frac{\Lambda_L}{\Lambda_O} < N < \frac{2\Lambda_L}{\Lambda_O} \qquad (9)$$

From Equation (8) and (9) it is found that inverted moiré magnification could be observed according to the following conditions:

(i) If the lens period Λ_L is larger than the object period Λ_O. For the same values of Λ_L and Λ_O inverted moiré magnification could be observed for different object positions depending on the value of N.

(ii) If the lens period Λ_L is smaller than the object period Λ_O. Inverted moiré magnification is only observed for N = 1 and $\Lambda_L < \Lambda_O < 2\Lambda_L$.

b) For $s_o = 2f$ (anti-principal planes position), the size of the object portion p_o is equal to the period of the lens array Λ_L, leading to m = -1. The composite image consists of locally inverted parts of the object. If the object period Λ_O is equal to the lens period Λ_L, a pattern similar to case III in Table 1 is observed.

c) For $\infty > s_o > 2f$, the size of the object portion p_o is larger than the pitch of the lens array Λ_L and -1 < m < 0. The lower limit for of the integer N ≥ 1 for a inverted demagnified moiré pattern is,

$$N > \frac{2\Lambda_L}{\Lambda_O}. \qquad (10)$$

6 Magnification

From the image equation (2) and Figure 3, the sign of the image portion p_i is positive or negative, corresponding to erect ($f > s_o > 0$) or inverted ($\infty > s_o > f$) imaging. From Equation (5) and (8), and the image equation (3), the magnification m of a moiré magnifier is always given by

$$m = \frac{\Lambda_L}{\Lambda_L - N\Lambda_O}. \qquad (11)$$

For erect imaging, the moiré image is always magnified (m > 1). For inverted imaging, the moiré image is either magnified (m < -1) or demagnified (-1 < m < 0).

7 Image formation and observation

In the simplest case, a lens array of L × L lenses and Λ_L lens period generates one complete magnified image of the object pattern (see Figure 1-d). In this case, the array size $L\Lambda_L$ is equal to the size of the moiré image. The object pattern has been magnified by factor m and we get the condition $L\Lambda_L = |m|\Lambda_O$. In a more general case, the lens array generates I × I magnified images of the object pattern, leading to

$$I = \frac{L\Lambda_L}{|m|\Lambda_O}. \qquad (12)$$

From Equation (11) and (12) the object period Λ_o is given by

$$\Lambda_o = \frac{L}{NL \pm I}\Lambda_L \qquad (13)$$

The positive sign holds for virtual erect images, the negative sign holds for inverted images. For $|\Lambda_L - N\Lambda_O| < \Lambda_L$ a magnified image is obtained. For $N\Lambda_O - \Lambda_L > \Lambda_L$ a demagnified image is obtained. Each value of Λ_O corresponds to a different object array position s_o given by

$$s_o = fN\frac{\Lambda_o}{\Lambda_L}. \qquad (14)$$

The size of the magnified image $m\Lambda_O$ is given by

$$m\Lambda_o = \frac{\Lambda_o}{\pm(\Lambda_L - N\Lambda_O)}\Lambda_L. \qquad (15)$$

The number of object patterns O, in one dimension, that contribute to one moiré image is equal to the magnification m,

$$O = |m|. \qquad (16)$$

The number of lenses L/I, in one dimension, that generate one moiré image is given by

$$\left|\frac{L}{I}\right| = \left|\frac{\Lambda_o}{p_o}\right| = \left|\frac{\Lambda_o}{\Lambda_L - N\Lambda_O}\right|. \qquad (17)$$

The moiré image generated by a moiré magnifier could be observed on a screen located at the image distance s_i, given by

$$s_i = -\frac{Nf\Lambda_O}{\Lambda_L - N\Lambda_O}. \qquad (18)$$

As a consequence of Equation (2), the moiré image can be observed by the naked eye at any position behind the lens.

For virtual erect moiré images, if the observer moves transversely to the lens array, the image appears to move in the same direction. For inverted moiré pattern, the image moves in the opposite direction. This corresponds to the sign of the magnification factor m as indicated in Equation (15).

A numerical example describing the generation of three different types of moiré images can be obtained by considering a moiré magnifier system consisting of a lens array period $\Lambda_L = 9u$ and object array of period $\Lambda_O = 4u$ where u is an arbitrary length-unit. Table 2 shows numerically the possible values of N satisfying the moiré magnifier inequalities (Equation (6), (9), and (10)), for $\Lambda_L / \Lambda_O = 9/4$.

$\Lambda_L = 9\,u$,			$\Lambda_o = 4\,u$		
Type of moiré image	Virtual erect magnified		Real inverted magnified		Real inverted demagnified
Condition N	$0 > N > \frac{9}{4}$		$\frac{9}{4} > N > \frac{13}{4}$		$\frac{13}{4} < N$
Condition s_o	$0 > s_o > -f$		$-f > s_o > 2f$		$-2f > s_o$
Value of N	a	b	a	b	5
	1	2	3	4	
Object array position s_o	$\frac{-4}{9}f$	$\frac{-8}{9}f$	$\frac{-12}{9}f$	$\frac{-16}{9}f$	$\frac{-20}{9}f$
Object array portion p_o	$5\,u$	$1\,u$	$3\,u$	$7\,u$	$11\,u$
The magnification M_T	$\frac{9}{5}$	9	$\frac{-9}{3}$	$\frac{-9}{7}$	$\frac{-9}{11}$

Table 2. Numerical example for a lens array period $\Lambda_L = 9$ u and object array period $\Lambda_L = 4$ u (arbitrary length-unit u). The table shows the possible values of N satisfying the moiré magnifier inequalities for $\Lambda_L / \Lambda_O = 9/4$.

For each value of N, the object position, s_o, and its corresponding object portion, p_o, and magnification, m, are calculated. Considering that the object array motif of the above moiré magnifier system consists of '1234', the Figures 5, 6 and 7 describe the generation of the different magnified images corresponding to different object array positions, s_o. Figure 5 shows the possible erect magnified moiré images, which are corresponding to the object array position, $0 < |s_o| < f$.
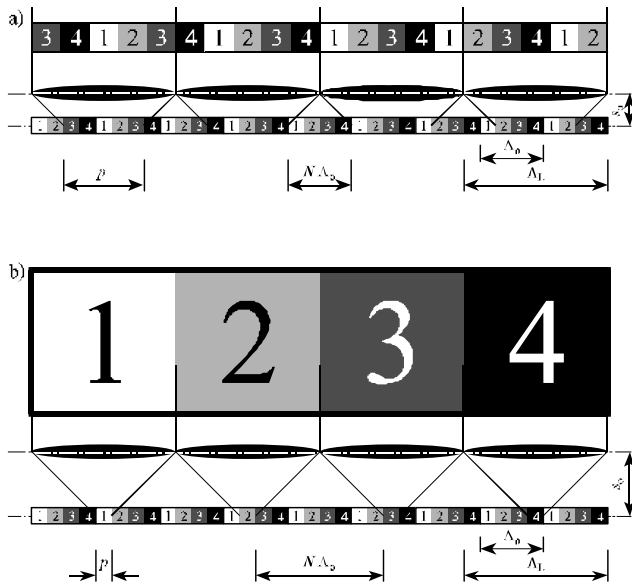

Figure 5. Erect magnified moiré images corresponding to the object array position, $0 < |s_o| < f$, and the value N = 1 (Figure 5-a) respectively N = 2 (Figure 5-b) as shown in Table 2.
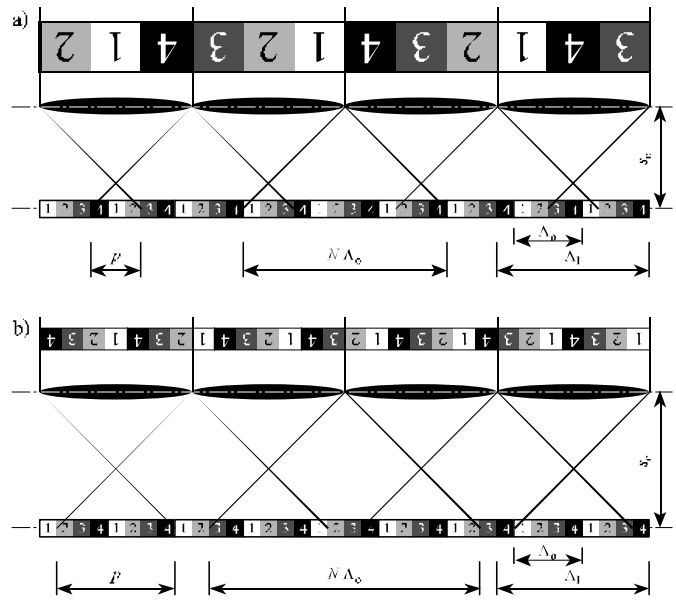

Figure 6. Inverted magnified moiré images corresponding to the object array position, $f < |s_o| < 2f$, and the value N = 3 (Figure 6-a) respectively N = 4 (Figure 6-b) as shown in Table 2.
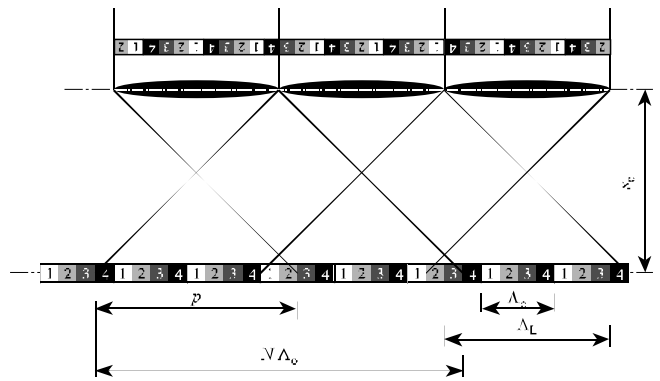

Figure 7. Inverted demagnified moiré image corresponding to the object array position, $2f < |s_o|$, and the value N = 5 as shown in Table 2.

Figure 5-a corresponds to N = 1, Figure 5-b to N = 2 as given in Table 2. Figure 6 shows the possible inverted magnified moiré images which are corresponding to the object array position, $f < |s_o| < 2f$. Figure 6-a corresponds to N = 3, Figure 6-b to N = 4. Figure 7 shows an inverted demagnified moiré image which corresponds with the object array position, $2f < |s_o|$ and N = 5.

The mathematical relations derived in this paper were confirmed experimentally. We have used a square lattice lens array of converging lenses. The size of the lens array is 42.73 mm², its period, Λ_L, is 1.07 mm, and the focal length, f, is 2.43 mm. Object arrays with different periods, Λ_o, are computer generated and printed onto transparency using a laser printer. The scheme of the experimental set-up is shown in Figure 8.
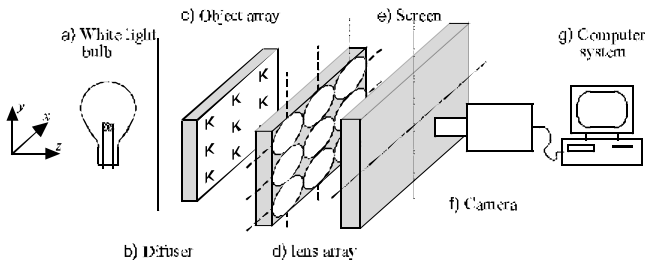
Figure 8. Experimental setup used for testing moiré magnifiers. The object array is placed in front of the lens array and illuminated by diffuse white light. The lens array is moved longitudinally in the z-direction and to adjust the object-to-lens distance, s_o. The real moiré images are projected on a screen and then recorded by a camera connected to a computer. In case of virtual moiré images, the images are received directly by the camera.

Diffused white light is used to illuminate the moiré magnifier system. The object array is placed in front of the lens array. The lens array is attached to a micro translation stage to move it longitudinally in the z-direction and to adjust the object array distance, s_o. The real moiré images are projected on a screen and then recorded by a camera connected to a computer. In case of virtual moiré images, the images are received directly by the camera. Table 3 shows the different object array periods, Λ_O, with their corresponding selected value of N, and positions, s_o. Also, the resulting magnification and image type are given for an aligned position. The experimental values are obtained from the recorded images. A selection of the resultant images is shown in Figure 9, 10, and 11.
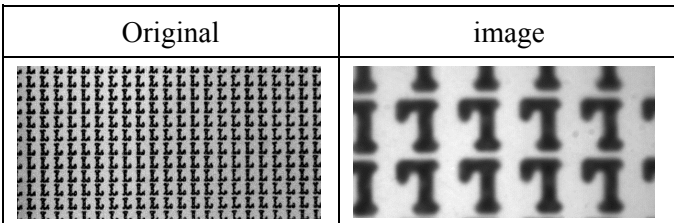

Figure 9. Object and image plane for a situation of real inverted magnified moiré patterns as described in Table 3.
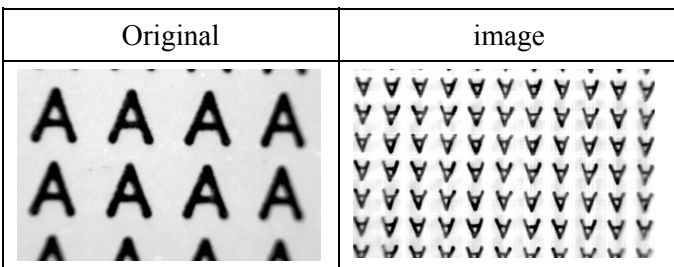

Figure 10. Object and image plane for a situation of real inverted demagnified moiré patterns as described in Table 3.
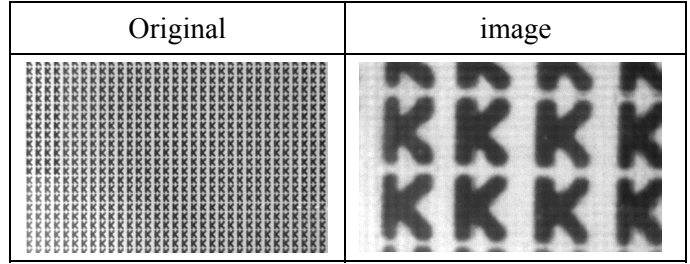

Figure 11. Object and image plane for a situation of virtual erect magnified moiré patterns as described in Table 3.

The object pattern is shown left, the observed moiré pattern on the right.

8 Translation and rotation

In the above analysis an aligned moiré magnifier is considered, that is, the axes of both object and lens array are parallel and coincident. If the lens is translated with respect to the object array, the moiré pattern appears to move. Each lens images another part of the related object. The direction of the movement depends on the relative motion of the arrays, the lens period, Λ_L, the object period, Λ_O, and the value of N, and is described by Equation (15). From the experiment it could be observed that for real moiré images, the resultant translation and rotation are in the same direction as those of the object array. While, it is in opposite direction for virtual patterns as we could expect from the sign of the magnification. The apparent motion speed of the resulted moiré image is proportional to the magnification value.

Moiré magnification is based on a periodically repeated object pattern imaged by a periodical array of identical lenses. The object period is the shortest distance between two identical parts of adjacent object unit cells along the lens array axes. Assume that we have an aligned configuration where moiré magnification appears. If the lens array (or the object array) is rotated by a small angle then the moiré image rotates and changes its magnification. For larger rotations, the moiré image might disappear and reappear at certain angles.

If one of the two arrays is rotated an angle Θ relative to the other, the distance to the next identical object part located on the lens axis will change. Accordingly, a new rectangular lattice of the object array, aligned with the lens array grid, with a new period is created at a certain rotation angle. The new period ratio, $\Lambda_L/\Lambda_{O,new}$, may satisfy or not moiré magnifier requirements at the same object array position, s_o. Therefore, moiré magnified images may appear and disappear as the object rotates.

Let assume a square grid of object with period Λ_O, that produces a moiré magnifier effect for a given position.
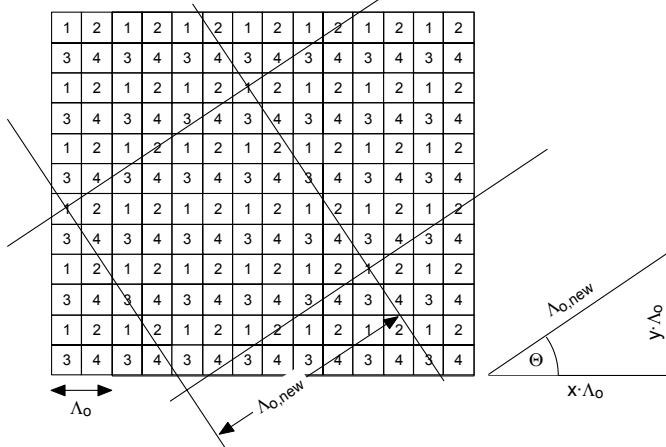

Figure 12. Rotation of the object array. A symmetric square array of identical objects ("1234") produces a new object period, $\Lambda_{O,new}$, for a rotation by an angle Θ.

A new square grid of repeated objects is obtained when the object rotates and the rotation angle obeys the following relation (see Figure 12),

$$\Theta = \tan^{-1}\left(\frac{y}{x}\right), \qquad (19)$$

where, x and y are integer numbers greater than, or equal, to zero (Θ changes from 0° to 90°). The new object array, aligned with the lens array, has a new pitch, which is equal to

$$\Lambda_{O,new} = \Lambda_O \frac{x}{\cos\Theta} = \Lambda_O \frac{y}{\sin\Theta} = \Lambda_O \sqrt{x^2 + y^2}. \qquad (20)$$

Thus, the varying rotation angles create new periods ratios, which define different moiré pattern characteristics.

An aligned position in which moiré magnification appears has a fixed value of *N*. If the distance between the two arrays remains unchanged then the imaged portion, p, will be the same although one of the two arrays rotates with respect to the other,

$$|p| = |\Lambda_L - N\Lambda_O| = |\Lambda_L - N_{new}\Lambda_{O,new}|. \qquad (21)$$

From this equation and Equation (20) the condition to obtain moiré magnification after rotation becomes,

$$N_{new} = \frac{N}{\sqrt{x^2 + y^2}} \qquad (22)$$

which is a very restricted condition to be fulfilled by the involved integer numbers. It is clear from Equation (11), that the magnification depends on the imaged portion and the lens pitch. So the magnification will keep constant for different rotation angles at the same object array position s_o.

9 Summary

If an array of identical lenses is used to view an array of identical objects, the phenomena of moiré magnification might occur. For certain array positions, a magnified image of the repeated object pattern is observed on a screen or by eye. The moiré image might be erect or inverted, magnified or demagnified. A shift in z or a rotation in θ of the lens array versus the object array might generate different magnified pattern. The object position in z and θ, which is necessary to observe a magnified moiré image is related to the difference in the array periods. A demagnified moiré image is observed, when the object period exceeds the lens period and the object array is located at a distance exceeding twice the focal length.

As one moves across the lens array, the moiré image appears to move in the same direction in case of virtual erect moiré pattern and in the opposite direction in case of real inverted moiré pattern.

The mathematical relations were in good agreement with the experiments performed for all three types of moiré magnified patterns.

10 Acknowledgement

11 References

1) M. E. Knotts, R. G. Hemphill, M. E. Knotts, "moiré or Moiré?", Optics & Photonics News, August 1996, 53-55 (1996).

2) O. Kafri, L. Glatt, "The physics of moiré metrology", Addison Wesly Publishing Company (1990).

3) G. Indebetouw, R. Czarnek, ed. "Selected papers on optical moire and applications", SPIE Milestone Series, Volume MS 64 (1992).

4) M. C. Hutley, R. F. Stevens and P. Savander, "The moiré magnifier", Pure Appl. Opt. 3, 133-142 (1994).

5) Mikami, Japan Journal of Applied Physics 14, 417-418 and 1065-1066 (1975).

6) N. Davies, M. McCormick, "The use of microlens arrays in integral photography", IOP Short Meetings No 30, Teddington, UK, 109-122 (1991).

7) N. Davies, M. McCormick, "Three dimensional optical transmission and micro optical elements", SPIE Vol. 1992 "Minature and Micro-Optics and Micromechanics", 247-257 (1993).

8) K. Hamanaka, H. Koshi, M. Toyama, "An artificial compound eye using a two-dimensional array of Selfoc lenses and its application to a scale-invariant image sensor", Technical Digest of MOC'95, Hiroshima, Japan, Optical Society of Japan, AP951224, 94-97 (1995).

9) J. S. Sanders, selected papers on "Natural and artificial compound eye sensors", SPIE Milestone Series Vol. 122 (1996).

10) W. Shaomin, L. Ronchi, "Principles and design of optical arrays", Progress in Optics XXV, 279-348 (1988).